

DESY 97-136
July 1997

Some Properties of the Very High Q^2 Events of HERA

Ursula Bassler, Gregorio Bernardi

Laboratoire de Physique Nucléaire et des Hautes Energies
Université Paris 6-7, 4 Place Jussieu, 75252 Paris, France
e-mail: bassler@mail.desy.de; gregorio@mail.desy.de

Abstract

The kinematic reconstruction of neutral current high Q^2 events at HERA is discussed in detail using as an example the recently published events of the H1 and ZEUS collaborations at $Q^2 > 15000 \text{ GeV}^2$ and $M > 180 \text{ GeV}$, which are more numerous than expected from Standard Model predictions. Taking into account the complete information of these events, the mass reconstruction is improved and the difference between the average mass of the samples of the two experiments is reduced from $26 \pm 10 \text{ GeV}$ to $17 \pm 7 \text{ GeV}$, but remains different enough to render unlikely an interpretation of the excess observed by the two collaborations as originating from the decay of a single narrow resonance.

arXiv:hep-ex/9707024v2 26 Jul 1997

1 Introduction

At the electron-proton (ep) HERA collider, the study of DIS is performed in an unique and optimal way up to values of the squared momentum transfer Q^2 of 10^5 GeV². Recently, the two HERA collaborations H1 and ZEUS have reported [1, 2] an excess of events at *very high* Q^2 (defined in the following as $Q^2 > 15000$ GeV²) compared to standard model expectations. This observation has triggered an important activity on “Beyond the Standard Model” theories which might explain the effect [3]. The most favoured solution involves the production of a new resonance, which after its decay is kinematically similar to a standard deep inelastic scattering (DIS) event.

Indeed, in the naive quark-parton model (QPM), a parton carrying a fraction x of the momentum of the proton scatters elastically against an electron and in the Standard Model, this interaction is representing a t-channel scattering occurring via the exchange of a gauge boson such as a photon or a Z^0 . Beyond the Standard Model, the naive QPM picture can represent the formation of an s-channel resonance (generically called “leptoquark”) subsequently followed by a two-body decay. While in the first interpretation the Bjorken x variable is one of the two relevant variables to characterize the scattering, in the second case the invariant mass M of the system formed is the physical quantity of interest. This mass is related to x in the naive QPM by $M = \sqrt{xs}$, s being the squared center of mass energy. In “real” interactions, the quantum chromodynamics (QCD) effects do not modify much this picture at large Q^2 , since it is characterized in DIS by the dominance of one electron + one partonic jet + one remnant jet in the final state, and is thus similar to the one in which a leptoquark is produced and decays in 2 bodies. So, when looking at high Q^2 deep inelastic scattering (DIS) in an inclusive way it is possible to distinguish between these two scenarios by comparing the event rates in different x or M intervals: the smooth evolution of the DIS cross-section as a function of x can be opposed to the appearance of a sharp peak in the invariant mass distribution, characteristic of a leptoquark.

The HERA effect is complicated by the fact that the invariant mass distributions of the event samples of the two collaborations differ: at a mass greater than 180 GeV, the 7 H1 events appear clustered around a mass of 200 GeV, while the 5 ZEUS events are broadly distributed between 191 and 253 GeV. It is the subject of this paper to understand how significant is this difference and to provide a combined mass spectrum using the complete available information of these events in order to give an interpretation of the effect.

At HERA the kinematic reconstruction does not need to rely on the scattered lepton only, since the most important part of the hadronic system is visible in the almost 4π detectors H1 and ZEUS. This redundancy allows for an experimental control of the systematic errors and the radiative corrections, hence to determine in a more precise way the usual DIS kinematic variables x, y and Q^2 which are defined as:

$$x = Q^2/(2P.q) \quad y = (P.q)/(P.k) \quad Q^2 = -(k - k')^2 = -q^2 = xys$$

P, k being the 4-vectors of the incident proton and lepton, k' the scattered lepton one.

In this report we briefly review in section 2 the methods used at HERA to determine the kinematics of the high Q^2 events. In section 3 we characterize the high Q^2 region and introduce a new method which optimizes the kinematic reconstruction by determining the measurement errors on an event by event basis. Section 4 is devoted to the detailed study of the very high Q^2 HERA events and discusses the mass distributions obtained.

2 Kinematic Reconstruction at HERA

In order to introduce the kinematic methods used at HERA in the high Q^2 region let us start by a few definitions. The initial electron and proton (beam) energies are labeled E_o and P_o . The energy and polar angle¹ of the scattered electron (or positron) are E and θ . After identification of the scattered electron, we can reconstruct the following independent hadronic quantities: Σ , obtained as the sum of the scalar quantities $E_h - p_{z,h}$ associated to each particle belonging to the hadronic final state, $p_{T,h}$ as its total transverse momentum and define the hadronic inclusive angle γ :

$$\Sigma = \sum_h (E_h - p_{z,h}) \quad p_{T,h} = \sqrt{(\sum_h p_{x,h})^2 + (\sum_h p_{y,h})^2} \quad \tan \frac{\gamma}{2} = \frac{\Sigma}{p_{T,h}} \quad (1)$$

$E_h, p_{x,h}, p_{y,h}, p_{z,h}$ are the four-momentum vector components of every energy deposit in the calorimeter originating from any hadronic final state particle. The corresponding quantities for the scattered electron are

$$\Sigma_e = E (1 - \cos \theta) \quad p_{T,e} = E \sin \theta \quad \text{i.e.} \quad \tan \frac{\theta}{2} = \frac{\Sigma_e}{p_{T,e}} \quad (2)$$

Out of these variables, it is possible to write the four methods which have been used to determine the invariant mass of the very high Q^2 events (the formulae are given in the appendix).

- The electron only method (e) based on E and θ .
- The hadrons only method (h) based on Σ and $p_{T,h}$ [4].
- The double angle method (DA) based on θ and γ [5].
- The Sigma method (Σ) based on E , θ and Σ [6].

The e method is precise at high y but becomes less precise in x, y or M at low y . The h method is the only one available for charged current events, but is less precise than the three others in neutral currents, so it will be ignored in the following. The DA method is precise at high Q^2 both at high and low y . The Σ method is similar to the e method at high y and to the DA at low y apart from Q^2 which is less precise. However it is insensitive to initial state QED radiation (ISR) in M, y and Q^2 . See [7] for a detailed discussion of the properties of these methods and [8] for their behaviour in presence of ISR.

¹The positive z axis is defined at HERA as the incident proton beam direction.

It should be stressed that the quality of any kinematic reconstruction depends mainly on the precision achieved on the observables, such as E , θ , Σ or γ . It is one of the major tasks of the experiments to obtain precise and unbiased quantities, and several techniques have been developed in the HERA structure function analyses to achieve these goals. We refer to the original publications for a description of these studies [9], which discuss for instance how the electron energy is calibrated, or how the hadronic final state is measured at low y , when the hadronic jets are in the vicinity of the beam pipe.

3 Treatment at High Q^2

At *high* Q^2 (defined in the following as $Q^2 > 2500 \text{ GeV}^2$) the kinematic reconstruction is in general more precise than at low Q^2 and indeed the differences between the results obtained with the methods seen above are small. However since the number of events drops rapidly with increasing Q^2 it is still crucial to optimize the reconstruction by making a full use of all the observables of these events.

The improvements on the reconstruction at high Q^2 come mainly from the better measurement of the hadronic final state. This is due to the fact that i) the individual hadron energy is on average greater; ii) the losses in the beam pipe and in the material in front of the calorimeter are in proportion smaller than at low Q^2 , i.e. Σ , $p_{T,h}$ and γ are less affected by these losses; iii) the hadronic final state displays more often a (single) collimated jet configuration. This is due both to kinematics (events are in average at higher x), and to the smaller gluon radiation and power corrections (α_S is smaller).

All these characteristics enable a precise measurement of the hadronic angle, and thus are particularly favourable to the DA method which indeed becomes more accurate with increasing Q^2 . This method has however the drawback to be very sensitive to ISR and it is thus difficult to apply to a small number of events. For instance, the ISR of a 2.75 GeV photon, if not taken into account produces a shift of 10% on the reconstructed mass and 20% on Q^2 . In order to overcome this drawback we introduce a new method which, by making use of the precision on γ , estimates *from the data* on an event by event basis the shift in the measurement of E and Σ , denoted in the following $\delta X/X \equiv (X_{true} - X_{reconstructed})/X_{reconstructed}$ with $X = E$ or Σ . These shifts allow i) the Σ method to be corrected; ii) the presence of an undetected initial state photon (down to an energy of about 2 GeV) to be identified with high efficiency, and therefore to correct for it.

3.1 The ω Method

Let us assume that there is no ISR (the specific treatment of ISR is discussed in the next section, although the two steps are not separated in the procedure), and that θ

and γ are precisely measured (implying $\delta\Sigma/\Sigma = \delta p_{T,h}/p_{T,h}$). From energy momentum conservation the two following equations can be derived:

$$(1 - y_e) \frac{\delta E}{E} + y_h \frac{\delta\Sigma}{\Sigma} = y_e - y_h \quad (3)$$

$$-p_{T,e} \frac{\delta E}{E} + p_{T,h} \frac{\delta\Sigma}{\Sigma} = p_{T,e} - p_{T,h} \quad (4)$$

Under these assumptions $\delta E/E$ and $\delta\Sigma/\Sigma$ are determined on an event by event basis. Varying θ and γ within their typical errors² (5 and 40 mrad (r.m.s.) respectively, at high Q^2) we can obtain the errors arising from the angular measurements on $\delta E/E$ and $\delta\Sigma/\Sigma$. A more direct way to see the uncertainties arising from this determination is illustrated in fig.1, in which the error on E and Σ reconstructed using equations 3 and 4 are compared to their “true” value, which is known for the reconstructed simulated events. For a given event, the error on $(\delta E/E)_{rec}$, which is defined as $\Delta(\delta E/E) \equiv (\delta E/E)_{rec} - (\delta E/E)_{true}$, is of the same order as the r.m.s. (denoted $\langle \delta E/E \rangle$) of the $\delta E/E$ distribution obtained from a large sample (fig.1b), showing that its use will not bring an improvement on an event by event basis. On the other side, the relative error on $(\delta\Sigma/\Sigma)_{rec}$ is smaller, about 30% of $\langle \delta\Sigma/\Sigma \rangle$, and diminishes at high y (compare fig.1e to 1f, and 1b to 1c) implying that correcting Σ will provide a better kinematic measurement, in particular at high y .

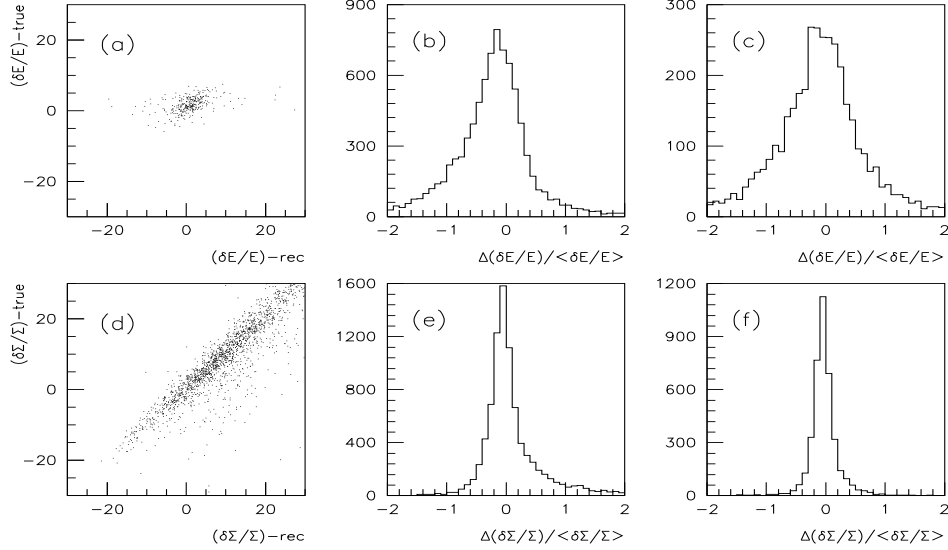


Figure 1: a) shows the correlation between true reconstruction errors on E and those obtained from eqs. 3 and 4, on a full simulation³ in the H1 detector of high Q^2 events; b) shows the projection of this correlation; c) shows the same projection restricted to $y > 0.4$. We use $\Delta(\frac{\delta E}{E}) \equiv (\frac{\delta E}{E})_{rec} - (\frac{\delta E}{E})_{true}$, and $\langle \frac{\delta E}{E} \rangle \equiv$ r.m.s. of the $\frac{\delta E}{E}$ distribution = 3%. d,e,f) show the same plots but for Σ instead of E , with $\langle \frac{\delta\Sigma}{\Sigma} \rangle = 10\%$.

²At very high Q^2 , the γ resolution improves to 30 mrad. We use here the r.m.s., rather than the standard deviation obtained from a gaussian fit to the distribution, to take into account non-gaussian tails which contribute in the propagation of the systematic errors.

The ω kinematic variables are thus derived from the Σ ones by including the effect of $\delta\Sigma/\Sigma$, i.e.

$$y_\omega \equiv \frac{\Sigma + \delta\Sigma}{\Sigma + \delta\Sigma + \Sigma_e} \quad Q_\omega^2 \equiv \frac{p_{T,e}^2}{1 - y_\omega} \quad (5)$$

The comparison of the ω and Σ reconstruction of M , y and Q^2 for high Q^2 events fully simulated³ in the H1 detector is shown in fig.2. The improvement obtained by the recalibration of Σ is clearly visible, allowing this method to be compared favourably to the original ones. This comparison is shown in fig.3 for high Q^2 events (in all the

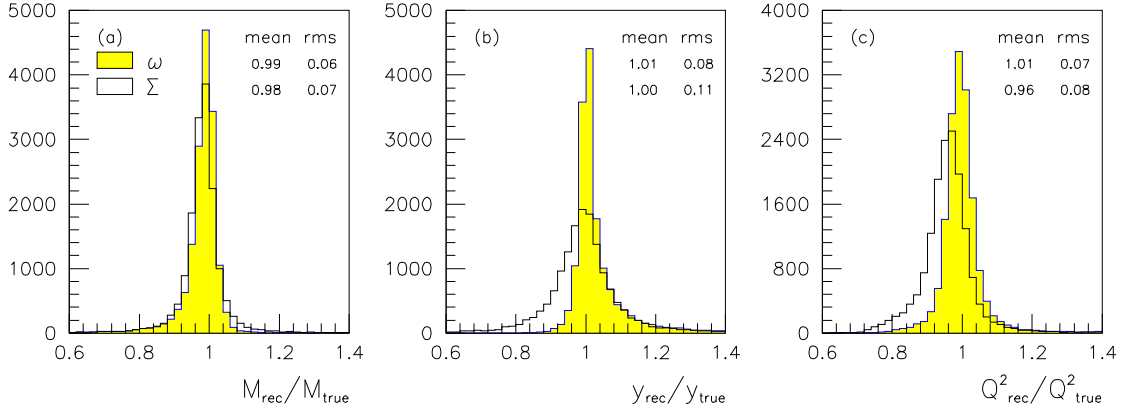


Figure 2: The improvements on the kinematic reconstruction at high Q^2 , when using the ω method compared to the Σ method, are shown for the mass M (2a), y (2b) and Q^2 (2c).

high Q^2 section, an $E - p_z$ cut against hard initial state radiation is applied, see next section) both at high y and at low y . At high y ($y_e > 0.4$), the e and the ω methods are comparable in M and y and slightly better than the DA one (fig.3a,b). In Q^2 , the DA displays the narrowest peak both at high and low y (fig.3c,f), but its high sensitivity to ISR induces tails in the distribution which renders its r.m.s. larger than the ω and e ones. At low y ($y_e < 0.25$) the e method has a relatively poor resolution in M , much worse than the ω one which is slightly better than the DA one. In conclusion, for the high Q^2 events the ω method is similar or slightly better than the e and DA method.

3.2 Treatment of QED Initial State Radiation

The influence of ISR is taken into account in the simulation programs used by the HERA experiments, but on a small number of events it is difficult to control the migration due to an unseen ISR photon when using the e and DA methods. Both H1

³In figures 1 and 2, the radiative processes of the DJANGO [10] program which is used to generate the events have been turned off. The complete simulation, based on DJANGO, ARIADNE [11] and GEANT [12] as used in the H1 simulation program, is further described in [1].

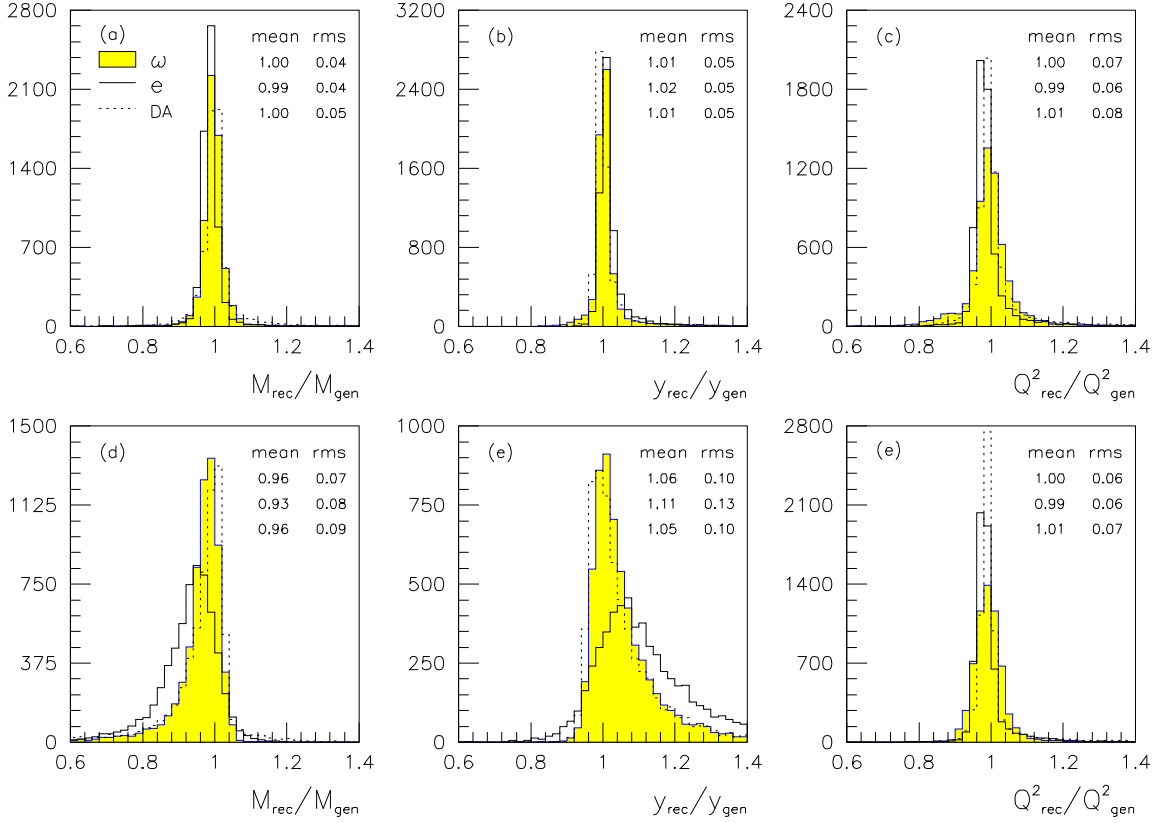


Figure 3: Comparison on high Q^2 events, at high y ($y_e > 0.4$) of the ω , DA and e reconstruction of the mass (3a), y (3b) and Q^2 (3c). The same comparisons are made at low y ($y_e < 0.25$) in fig. 3d,e,f.

and ZEUS use an experimental cut on the total $E - p_z$ of the event (Σ_{he}) or equivalently on the normalized $E - p_z$ called hereafter σ_{he} ⁴ and defined as

$$\sigma_{he} \equiv \frac{\Sigma_{he}}{2E_o} \equiv \frac{\Sigma + \Sigma_e}{2E_o} \equiv \sigma_h + \sigma_e \quad (6)$$

The $E - p_z$ cuts used in H1 and ZEUS correspond to good approximation to $\sigma_{he} > 0.75$ and prevent an ISR photon from carrying away more than about 25% of the incident electron energy. Such a photon can induce a large shift to the reconstructed mass [8] of $1 - \sqrt{(0.75y_e)/(y_e - 0.25)}$ for M_e (i.e. -18% at $y_e = 0.75$) and of 25% on M_{DA} at any y . On M_Σ the shift is zero since the method is independent of colinear ISR for M , y and Q^2 . A more stringent cut on σ_{he} is difficult to implement due to the experimental resolutions on y_h and y_e .

The ω method allows ISR to be identified with high efficiency for σ_{he} as high as ~ 0.93 . It makes use of the simple fact that depending on the origin of the σ_{he} shift (which comes mainly either from ISR or from hadronic miscalibration), the errors

⁴The normalized $E - p_z$ for the electron and for the hadronic final state satisfy: $\sigma_e = 1 - y_e$; $\sigma_h = y_h$.

obtained with the ω method have a completely different pattern: for example if the observed σ_{he} is $1-z$, equations 3 and 4 will give for the ISR case $\delta E/E = z$ and $\delta\Sigma/\Sigma = z$, assuming negligible detector smearing, while for the hadronic miscalibration case, assuming negligible error on the electron energy, we will get $\delta E/E = 0$ and $\delta\Sigma/\Sigma = z/y_h$. These two different types of pattern allow ISR to be identified even in the presence of detector smearing, as studied on a complete simulation in the H1 detector, with typically 85% efficiency at high Q^2 for photon energies greater than 2 GeV. The exact conditions for ISR identification of a 2 GeV photons is $\delta E/E$ and $\delta\Sigma/\Sigma > 7.3\%$. However, to take into account the detector smearing we use instead:

$$\frac{\delta E}{E} > 5\% \quad \text{and} \quad \frac{\delta\Sigma}{\Sigma} > 5\% \quad \text{and} \quad \frac{\delta E}{E} + \frac{\delta\Sigma}{\Sigma} > 15\% \quad (7)$$

These can be slightly varied depending on the ISR identification efficiency requested. These conditions will “misidentify” high Q^2 non-radiative events in less than 3% of the cases in the H1 detector, implying that in the total sample of ISR identified events, the fraction of genuine ISR events is higher than the fraction of non-radiative events. This fraction increases with increasing Q^2 since the hadronic angle becomes more precise, i.e. the ISR identification becomes more efficient. In case of ISR identification, the equations 3 and 4 are solved again after recalculating y_e and y_h using $\sigma_{he} \cdot 2E_o$ instead of $2E_o$. The improvement obtained can be visualized in fig.4 which shows the same distributions as in fig.3 but on the sample of DIS high Q^2 events having radiated an ISR photon of 2 GeV or more. The dramatic improvement underlines the importance of controlling experimentally the radiation effect. Furthermore, the soft ISR photons which cannot be identified below 2 GeV have a small effect on M_ω ($< 2\%$) but still a sizeable one on M_{DA} , up to about 7%, or 4% on M_e .

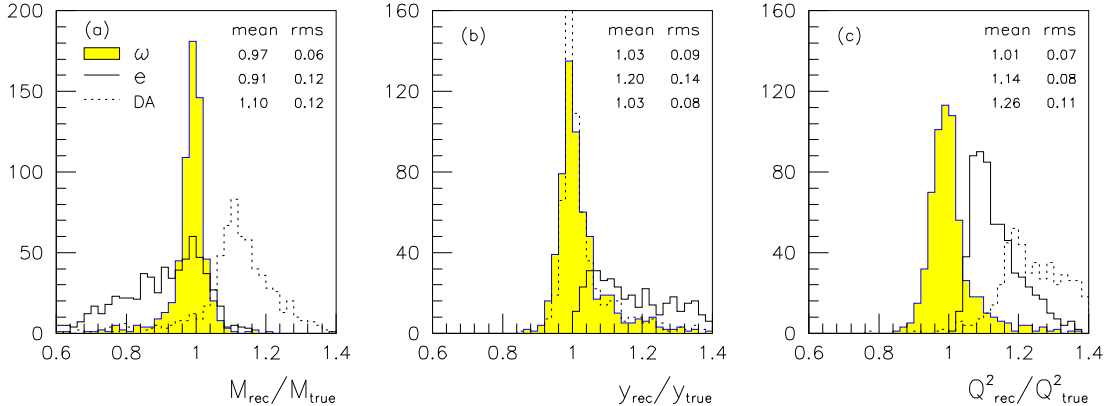


Figure 4: Comparison of the ω, e and DA reconstruction of the mass (4a), y (4b) and Q^2 (4c) for high Q^2 radiative events in which $E_\gamma^{ISR} > 2$ GeV (and $\sigma_{he} > 0.75$). Note the similar behaviour of y_ω and y_{DA} , since y_{DA} is ISR independent. In M and Q^2 the improvements brought by the ω reconstruction method are remarkable.

4 The Very High Q^2 Events at HERA

Let us remind some characteristics of the excess of events at high Q^2 observed by the H1 and ZEUS collaborations in the data collected from 1994 to 1996 [1, 2]. At $Q^2 > 15000$ GeV², 24 events have been observed for an expectation of 13.4 ± 1.0 , representing a probability of 0.0074 [13]. Furthermore some of these events exhibit the additional characteristics either to cluster around a rather precise value of the invariant mass of the produced system ($M_e = 200 \pm 12.5$ GeV, for 7 events out of the 12 of H1, while 1.0 ± 0.2 are expected), or to lie at very high invariant mass ($M_{DA} > 223$ GeV and $y_{DA} > 0.25$, for 4 events out of the 12 of ZEUS, while 0.9 ± 0.2 are expected). Actually the messages of these two observations could be different as already pointed out [14, 15] and we will try here to explore further this point with the use of our new kinematic tool.

Among the obvious possible reasons for the difference are the influence of ISR which can strongly distort a distribution based on a small number of events, or the effect of a specific miscalibration. The ω method having been devised to respond to these problems, we can now study in more details the 11 extreme events mentioned above for which the complete kinematic information has been published by the two collaborations. We add to this sample 2 events⁵ from ZEUS in order to include all events which satisfy the condition $Q^2 > 15000$ GeV² and $M > 180$ GeV, since we want to test the significance of the H1 event clustering at masses around 200 GeV over the complete very high Q^2 HERA sample.

4.1 Kinematic Properties

In table 1 are given the M , y and Q^2 of the 13 events at very high Q^2 and high mass reconstructed with the four different methods discussed above. The values of M , y and Q^2 are identical to those published for the e and DA methods. The Σ values have been released recently by H1 [16] and can be computed straightforwardly for the ZEUS events. The errors are also reproduced exactly except for those of the e method to which we conservatively added quadratically an error of 1.5% (i.e. half of the absolute energy scale uncertainty of 3% given by the two experiments) to account for potential miscalibrations between the different regions of the detectors. As we will see below the overall energy calibration can be checked to be well under control.

For the errors not published by the collaborations (ω , Σ for H1 and ZEUS, and DA for H1) we used the following prescription, which was checked to be consistent with the other published errors: They are obtained here using a possible error of ± 5 mrad and ± 30 mrad for the electron and hadronic angle respectively. For the error on the

⁵For one of these 2 events (called Z-6 in table 1) only the DA variables are available (from fig.1 of ref. [2]). The additional kinematic properties were deduced from the DA values using the average $E - p_z$ and systematic shifts between e and DA variables of the 5 other ZEUS published events. This assumption has a negligible influence on the conclusions drawn below.

electron (hadronic) energy we used $\pm 3\%$ ($\pm 4\%$) for H1 and $\pm 5\%$ ($\pm 4\%$) for ZEUS, which includes for the electron case both resolution effects, dead material corrections and the 1.5% overall error just mentioned. These two values for the electron energy error have been checked on the data (see below). Additional sizeable errors as published by the collaborations, due for instance to special energy corrections, have been taken into account in two events (H-3,Z-1).

For the H1 events the errors of an event are similar for each method, with a slight advantage for the e method at y above 0.5. For the ZEUS events the DA errors are the smallest, since the error on the electron energy which is somewhat larger than in the H1 case has an influence on the 3 other methods. This also explains why the ZEUS collaboration chooses the DA method rather than the e method favoured by H1.

Also mentioned is the result of the ω ISR identification, and we can see that 2 events (H-5 and Z-4) are classified as radiative, and have been corrected accordingly. These 2 events indeed show the characteristics of a radiative event, i.e. there exists a value of $z \equiv E_\gamma^{ISR}/E_o$ for which the following equations, which hold exactly if there were no detector effects, are verified in a good approximation:

$$\delta E/E \simeq z \quad \delta \Sigma/\Sigma \simeq z \quad (8)$$

$$Q_\Sigma^2/Q_e^2 \simeq 1 - z \quad Q_e^2/Q_{DA}^2 \simeq 1 - z \quad (9)$$

$$M_\Sigma/M_{DA} \simeq 1 - z \quad x_\Sigma/x_{DA} \simeq (1 - z)^2 \quad (10)$$

$$y_{DA} \simeq y_\Sigma \quad \sigma_{he} \simeq 1 - z \quad (11)$$

Indeed in the case of H-5 a photon with an energy (2.9 GeV) consistent with the z derived from the previous equations is observed in the special photon calorimeter located close to the beam pipe and designed to measure photons emitted collinearly to the incident electron, such as ISR photons. The ISR effect on the mass is sizeable, since $M_{DA}/M_\omega = 1.08$ for H-5 and 1.11 for Z-4. Both values are consistent with the determined $\delta E/E$ and $\delta \Sigma/\Sigma$ of these events (see tab.1).

The reconstructed kinematics are consistent between the different methods except for the 2 radiative events and for the events displaying a significant difference between M_e and M_{DA} (events H-7,Z-1,Z-5), which indeed have the largest $\delta E/E$ and/or $\delta \Sigma/\Sigma$.

On these small samples of events, and after ISR corrections, the averages of the absolute value of the error on the hadronic energy are similar for H1 and ZEUS ($\langle |\frac{\delta \Sigma}{\Sigma}| \rangle = 6\%$ compared to 5%), while on the electron energy the H1 average error is smaller: $\langle |\frac{\delta E}{E}| \rangle = 3\%$ compared to 5% for ZEUS.

The uncertainty on the electromagnetic absolute energy scale can be estimated *from the data* using $\langle \frac{\delta E}{E} \rangle$ (the 2 radiative events are excluded from these means) which gives $+1.1\% \pm 1.5\%$ for H1 and $+2.1\% \pm 3\%$ for ZEUS, both values in good agreement with the value of 3% given by the collaborations. The uncertainty on the hadronic absolute energy is obtained similarly and gives $-5.4\% \pm 3\%$ for H1 and $+3.3\% \pm 4\%$ for ZEUS, also in acceptable agreement with the values quoted by the collaborations.

After all these consistency checks, the use of the ω method in the two samples will now allow a consistent mass distribution to be derived from the very high Q^2 events.

Evt	$\frac{\delta E}{E}$	M_ω	M_{DA}	M_e	M_Σ	y_ω	y_{DA}	y_e	y_Σ	Q_ω^2	Q_{DA}^2	Q_e^2	Q_Σ^2
σ_{he}	$\frac{\delta \Sigma}{\Sigma}$	δM_ω	δM_{DA}	δM_e	δM_Σ	δy_ω	δy_{DA}	δy_e	δy_Σ	δQ_ω^2	δQ_{DA}^2	δQ_e^2	δQ_Σ^2
H-1	+0.01	197	198	196	196	.435	.434	.439	.443	16.8	17.1	17.0	17.1
1.01	-.03	7	7	6	7	.016	.016	.016	.032	0.9	0.5	0.5	1.2
H-2	-.04	208	200	208	209	.574	.582	.563	.592	24.8	23.3	24.4	25.9
1.06	-.07	6	5	5	6	.013	.013	.014	.024	1.2	0.8	0.5	1.8
H-3	-.01	188	185	188	188	.568	.573	.566	.561	20.0	19.6	20.0	19.7
0.99	+0.03	12	5	12	12	.020	.012	.033	.028	2.0	0.6	1.4	2.2
H-4	+0.02	197	199	198	196	.789	.787	.790	.786	30.7	31.3	30.9	30.2
0.98	+0.02	4	4	3	5	.009	.007	.009	.012	1.2	1.1	0.7	1.7
H-5	+0.08*	210	227	211	210	.525	.526	.562	.525	23.1	27.1	25.0	23.1
0.92*	+0.08*	6	7	5	6	.015	.016	.014	.031	1.2	0.9	0.5	1.8
H-6	+0.00	193	190	192	190	.440	.443	.440	.501	16.3	16.1	16.1	18.1
1.12	-.22	6	6	7	6	.015	.016	.018	.030	0.9	0.5	0.5	1.3
H-7	+0.10	199	213	200	202	.778	.762	.783	.786	30.7	34.5	31.4	31.9
1.02	-.05	5	5	3	6	.009	.008	.009	.013	1.2	1.3	0.7	2.0
Z-1	-.07	221	208	218	207	.856	.865	.854	.836	41.7	37.5	40.5	35.9
0.89	+0.17	10	8	10	12	.011	.008	.018	.019	3.4	2.6	3.2	4.5
Z-2	+0.03	220	227	220	220	.497	.490	.505	.507	24.1	25.2	24.4	24.6
1.00	-.04	11	6	10	11	.019	.010	.025	.034	1.9	0.7	1.2	2.4
Z-3	+0.02	228	236	225	230	.306	.299	.319	.299	15.9	16.6	16.2	15.8
0.97	+0.03	14	10	21	17	.023	.017	.040	.042	1.4	0.5	0.9	1.6
Z-4	+0.12*	227	253	233	228	.728	.721	.752	.731	37.5	46.1	41.0	37.8
0.92*	+0.07*	9	6	12	10	.014	.008	.021	.021	2.5	1.6	3.1	3.4
Z-5	+0.10	207	232	200	206	.305	.285	.350	.310	13.1	15.4	14.0	13.2
0.94	-.03	13	10	15	15	.024	.017	.033	.044	1.2	0.4	0.7	1.4
Z-6	+0.03	185	191	186	183	.608	.592	.610	.591	20.7	21.6	21.0	19.8
0.95	+0.07	12	11	12	12	.023	.028	.054	.054	2.1	1.6	1.5	3.2

Table 1: Kinematic properties of the 13 events observed by the H1 and ZEUS collaborations which have, at least in one method, $Q^2 > 15000 \text{ GeV}^2$ and $M > 180 \text{ GeV}$. For event Z-6, only the DA values are accurate, the values of the other methods being extrapolated. The values of M , y and Q^2 are identical to those of the original papers (e , DA , Σ for H1 [1, 16], e , DA for ZEUS [2]). The new values of the table are for the Σ (ZEUS) and for the ω (H1+ZEUS), and for the non available errors (see text for more details). Also given are σ_{he} , $\frac{\delta E}{E}$ and $\frac{\delta \Sigma}{\Sigma}$, which allow to quantify the size of the errors and to tag the presence of initial state radiation and to correct for it (marked with a “*”). After ISR corrections, the $(\sigma_{he}, \frac{\delta E}{E}, \frac{\delta \Sigma}{\Sigma})$ values are for event H-5: (1.00,.00,.00) and for event Z-4: (1.00,+0.04,-.01). The masses are given in GeV, the Q^2 in 10^3 GeV^2 .

4.2 Mass Distribution

In the following we will not consider any more the event Z-5, since it survives the Q^2 cut only for the DA method. It might be a radiative event which could not be identified due to a large smearing in the hadronic energy. In any case (radiative or not) it would not survive the Q_ω^2 cut, which is one of the 2 conditions the final sample must satisfy. Note “en passant” that its mass is reduced from $M_{DA}=232$ GeV to $M_\omega=207$ GeV. The mass distributions of the remaining 12 events, obtained with the e , DA, Σ and ω , are displayed in fig.5a,b,d,e.

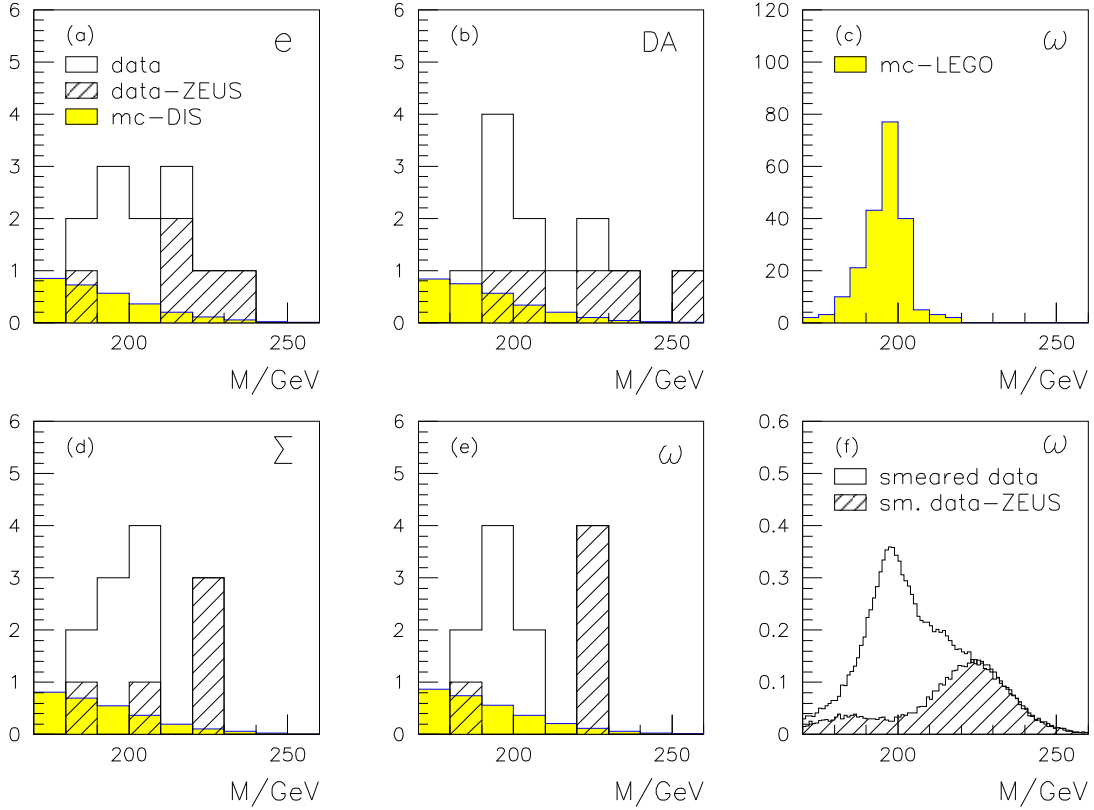


Figure 5: Mass distributions obtained with the e (5a), DA (5b), Σ (5d) and ω (5e) reconstruction methods. The main histogram represents the mass distribution of the H1 and ZEUS events at $Q^2 > 15000$ GeV² and $M > 180$ GeV². The dashed histogram represents the contribution of the ZEUS events only. The grey histogram represents the prediction from Standard Model DIS, obtained from a simulation normalized to the summed luminosity of H1 and ZEUS. Fig.5c displays the ω mass reconstruction of a 200 GeV narrow resonance generated with the LEGO program [17] and fully simulated in the H1 detector. Fig.5f is obtained from fig.5e by filling one gaussian distribution per event, with mean and width given by its ω -mass and its error (cf table 1).

The event Z-4 has the highest mass at 253 ± 6 GeV. It is identified as a radiative event and its mass is reduced by the ω determination to 226 ± 5 GeV, thereby reducing the scattering appearance of the ZEUS events. Note that the error quoted on the DA mass is much smaller than the effect due to radiation.

For the 5 ZEUS events the weighted average mass is decreased from $M_{DA}^{avg}=226 \pm 9$ GeV to $M_{\omega}^{avg}=216 \pm 7$ GeV. Actually with the ω determination 4 out of the 5 ZEUS events lie between 220 and 228 GeV, the 5th one (Z-6) being at 185 GeV, i.e. at a lower mass than any of the 7 H1 events (see fig.5b).

The average mass⁶ of the 7 H1 events is essentially not dependent on the method used: $M_{\omega}^{avg}=199 \pm 2.5$ GeV, $M_e^{avg}=200 \pm 2.6$ GeV, $M_{DA}^{avg}=201 \pm 5$ GeV. The 7 H1 events remain clustered between 188 and 211 GeV. Thus the H1 and ZEUS samples are concentrated at significantly different mass values and this splitting cannot be accounted for either by ISR or by detector effects.

The small number of events involved prevents a definite interpretation of this effect. However the fact that no event among the 5 of ZEUS is found in the bin where the 7 H1 events are measured suggests that this specific accumulation is a statistical fluctuation. In fig.5c is shown the reconstruction of a narrow resonance generated at $M=200$ GeV with the LEGO [17] program in the H1 detector using the ω method⁷. The width of the distribution which include experimental and QED/QCD radiation effects, cannot accomodate the tails of the measured experimental distributions (fig.5a,b,d,e).

If we make an ideogram from the histogram 5e i.e. if we apply gaussian smearing to each of the 12 events using their ω mass as a mean, and their error as r.m.s., we obtain fig.5f, which also shows the incompatibility with fig.5c. To reconcile the 2 “peaks” visible in fig.5f would require to miscalibrate uniformly the electron energy of the H1 events at least by +6% and the ZEUS events by -6%, values completely incompatible with the absolute scale uncertainties found in the previous section. Note however, that the H1 events alone support the narrow resonance hypothesis.

Since after the ω kinematic treatment none of the 12 events migrates outside the very high Q^2 and mass region, we confirm that the visible excess published by the collaborations at very high Q^2 is not due to detector (calibration) or radiation (ISR) effects.

⁶ The fact that the average masses are slightly different from the original publications is due to the difference in the errors which weights the events in a different way. This difference is irrelevant in the current discussion.

⁷All the methods give similar distributions on these events, except for the DA which has a larger r.m.s. due to radiative tails. In units of GeV the (mean; r.m.s.) are for the ω , e , DA and Σ respectively: (195.5; 7.5), (195.3; 7.4), (195.2; 9.6), (195.3; 7.8). The bias of about 5 GeV can be removed by taking into account the mass of the jet, but is present when using inclusive methods.

5 Conclusion

We have introduced a new reconstruction method (“ ω ”) which allows the kinematic variables of the high Q^2 events to be determined in a more precise way. It uses the kinematic constraints on an event by event basis to calibrate the hadronic energy and to identify and correct for the presence of QED initial state radiation.

This method has been applied to the 12 HERA events observed by the H1 and ZEUS collaborations (for an expectation of about 5) at $Q^2 > 15000 \text{ GeV}^2$ and $M > 180 \text{ GeV}$. The accumulation of the 7 H1 events around $200 \pm 12.5 \text{ GeV}$ is confirmed. The average mass of the 5 ZEUS events is decreased from the double-angle value of $226 \pm 9 \text{ GeV}$ to $216 \pm 7 \text{ GeV}$. However none of the ZEUS events enter the H1 accumulation region. Taking the estimation of the systematic errors at face value, this suggests that, if the observed excess at very high Q^2 is due to physics beyond the Standard Model, it is unlikely to be explained by the decay of a single narrow resonance such as a leptoquark. The increase of the integrated luminosity in the current and in the future years at HERA will clarify the origin of this effect.

Acknowledgments

We would like to thank the two collaborations for the data we have studied in this paper. In particular this work has taken place within the H1 collaboration, and some of the results obtained were the outcome of the efforts of many people of the “Beyond the Standard Model” group to get the analysis of the very High Q^2 events completed. We also would like to thank J. Dainton, R. Eichler, J. Gayler, D. Haidt, B. Straub and G. Wolf for a careful reading of the manuscript and for their useful remarks.

Appendix: y and Q^2 formulae ($M \equiv \sqrt{Q^2/y}$)

method	y	Q^2
e	$1 - \frac{E}{E_0} \sin^2 \frac{\theta}{2}$	$\frac{p_{T,e}^2}{1-y_e}$
h	$\frac{\Sigma}{2E_0}$	$\frac{p_{T,h}^2}{1-y_h}$
DA	$\frac{\tan \frac{\gamma}{2}}{\tan \frac{\gamma}{2} + \tan \frac{\theta}{2}}$	$4E_0^2 \frac{\cot \frac{\theta}{2}}{\tan \frac{\gamma}{2} + \tan \frac{\theta}{2}}$
Σ	$\frac{\Sigma}{\Sigma + E(1 - \cos \theta)}$	$\frac{p_{T,e}^2}{1-y_\Sigma}$

References

- [1] H1 Collab., C. Adloff et al., Z. Phys C74 (1997) 191.
- [2] ZEUS Collab., J. Breitweg et al., Z. Phys C74 (1997) 207-220.
- [3] Yu. L. Dokshitzer, and references therein, to appear in the Proceedings of the 5th International Workshop on Deep Inelastic Scattering and QCD, Chicago (1997).
- [4] A. Blondel, F. Jacquet, Proceedings of the Study of an *ep* Facility for Europe, ed. U. Amaldi, DESY 79/48 (1979) 391-394.
- [5] S. Bentvelsen et al., Proceedings of the Workshop Physics at HERA, vol. 1, eds. W. Buchmüller, G. Ingelman, DESY (1992) 23-40.
C. Hoeger, *ibid.*, 43-55.
- [6] U. Bassler, G. Bernardi, Nucl. Instr. and Meth. A361 (1995) 197.
- [7] U. Bassler, G. Bernardi, DESY 97-137 (1997)
- [8] G. Wolf, hep-ex/9704006, DESY 97-047 (1997) 26.
- [9] H1 Collab., T. Ahmed et al., Nucl. Phys. **B439** (1995) 471.
ZEUS Collab., M. Derrick et al., Z. Phys. **C65** (1995), 379.
H1 Collab., S. Aid et al., Nucl. Phys. **B470** (1996) 3.
ZEUS Collab., M. Derrick et al., Z. Phys. **C72** (1996) 399.
- [10] G. A. Schuler and H. Spiesberger, Proceedings of the Workshop Physics at HERA, vol. 3, eds. W. Buchmüller, G. Ingelman, DESY (1992) 1419.
- [11] L. Lönnblad, Computer Phys. Comm. **71** (1992) 15.
- [12] R. Brun et al., GEANT3 User's Guide, CERN-DD/EE 84-1, Geneva (1987).
- [13] Joint H1+ZEUS table of high Q^2 events. Private communication.
- [14] M. Drees, hep-ph/9703332, APCTP 97-03 (1997) 5.
- [15] G. Altarelli et al., hep-ph/9703276, CERN-TH/97-40 (1997) 28.
- [16] G. Bernardi, T. Carli, to appear in the Proceedings of the 5th International Workshop on Deep Inelastic Scattering and QCD, Chicago (1997).
- [17] K. Rosenbauer, Ph.D thesis RWTH Aachen, PITHA-95/16 (1995).